JOURNAL OF CATALYSIS 91, 85–92 (1985)

The Role of Excess Antimony as a Promoter of Activity and Selectivity in Selective Oxidation in the Fe–Sb System

M. CARBUCICCHIO, G. CENTI,* AND F. TRIFIRÒ*,[1]

*Istituto di Fisica dell'Università di Parma, Parma, Italy, and *Istituto di Tecnologie Chimiche Speciali, Via Risorgimento 4, 40136 Bologna, Italy*

Received February 1, 1984; revised June 14, 1984

The modifications of two iron–antimony oxides with Sb–Fe ratios of 1 and 2 during calcination up 1000°C and after catalytic tests (1-butene oxidation to butadiene) were studied by X-ray diffraction, infrared, and Mössbauer analyses. The results show that a nonstoichiometric (NS) rutile structure with excess antimony held within the structure itself is formed on both catalysts calcined up to 900°C. The strong increase both in selectivity and activity in allylic oxidation showed by the catalyst with an Sb : Fe ratio of 2 is attributed to the formation of a NS-rutile that is stable during catalytic tests. It is suggested that the excess antimony held within the structure creates Sb=O double bonds which are responsible for the increase of selectivity and activity. The fundamental role of the method of preparation by coprecipitation in a basic medium is also suggested.

INTRODUCTION

As is well known, iron–antimony mixed oxides are active and selective catalysts for the allylic oxidation and ammonoxidation of olefins. The Fe_2O_3–Sb_2O_4 system has been widely studied at different Sb/Fe ratios and it has been found that (i) by increasing the Sb/Fe ratio from about 0.8–1.0 to 1.8–2.0, the specific rate and the selectivity drastically increase and (ii) $FeSbO_4$ was the only mixed oxide for all compositions found.

Different opinions have been advanced in the literature on the role of the excess antimony in improving the catalytic behavior toward selective oxidation. Boreskov *et al.* (*1, 2*) proposed that the excess antimony avoids the formation of free Fe_2O_3 which can be responsible for the total oxidation. Fattore *et al.* (*3*) assumed that an active and selective species forms at the grain boundary between Sb_2O_4 and $FeSbO_4$. Sala and Trifirò (*4*) suggested the formation of $Fe(II)Sb_2O_6$ on the surface of catalyst with an Sb/Fe ratio of 2, of Sb(V)=O bonds similar to those present in Sb_2O_5 and of Fe–Sb–Sb–Fe species (*4*). In agreement with this, Aso *et al.* (*5, 6*) suggested that the excess antimony forms a particular surface structure with an Sb-enriched composition on the top of the $FeSbO_4$. The formation of a Fe(II) species in the Fe–Sb system has been observed by many authors (*6–10*). Burriesci *et al.* (*7*) hypothesize that the excess antimony is important only during preparation, where it promotes the formation of Fe(II) and oxygen vacancies in the $FeSbO_4$ structure. For Kriegsmann *et al.* (*8*) the excess antimony induces modifications in the M–O covalent bond strength. Recently Dziewiecki and Makowski (*11*) suggested that a solid solution can occur between $FeSbO_4$ and antimony in excess.

The aim of the research reported in this paper was to further the knowledge of the role of excess antimony in improving the catalytic behavior of Fe–Sb mixed oxides. Some discordances found in the literature can be due to the method of preparation which, in many cases, allowed only partial reaction between the components, so that mixed oxides could coexist with the pure oxides (*7*). In contrast, the coprecipitation

[1] To whom correspondence must be sent.

0021-9517/85 $3.00

technique we adopted allows very homogeneous and reproducible mixed compounds to be obtained. In this way a better understanding of the physical-chemical nature of the catalyst is possible. The chemical modification of the catalysts over a wide range of temperatures was studied using different techniques.

EXPERIMENTAL

Sample Preparation and Characterization

The samples with atomic ratio Sb : Fe = 1 (SbFe 1) and Sb : Fe = 2 (SbFe 2) were prepared by coprecipitation technique: dissolving $FeCl_3 \cdot 6H_2O$ (Carlo Erba RPE) in water, adding $SbCl_5$ (Carlo Erba RPE) in the required quantities to obtain the desidered Sb : Fe ratios, and neutralizing the solution with ammonia to pH 8. After it was dried overnight at 130°C, the precipitate was calcined in air for 15 h at 350°C and then in successive steps at 600, 800, 900, and 1000°C for 1 h 30 min at each step.

X-Ray diffraction patterns were recorded with a Rich Seiffert diffractometer using Ni-filtered Cu$K\alpha$ radiation. The (110), (101), (200), (211), and (220) lines of the rutile structure were used to determine the lattice parameters.

Infrared transmission (T) and diffuse reflectance (DR) spectra were run on a Model A202 Jasco infrared spectrometer equipped with a diffuse reflection attachment DR-31; the samples were diluted in both cases with KBr.

Mössbauer absorption spectra of the ^{57}Fe 14.4-keV radiation were measured by means of a constant acceleration spectrometer and a source of 25-mCi ^{57}Co in a Rh matrix. The spectra were fitted by superimposing a series of Lorentzian lines.

Catalytic Measurements

Catalytic tests were carried out on the catalysts (SbFe 1 and SbFe 2) calcined at 900°C. The catalytic activities were measured in an isothermal fixed-bed conventional flow reactor at atmospheric pressure. The reactor consisted of a stainless-steel tube (4 mm diameter, 300 mm long) placed in a copper bar and externally electric resistance heated. An axial thermocouple was inserted inside the catalytic bed. The feed composition (%vol) was 0.606 : 11.1 : 88.3 1-butene : oxygen : nitrogen, respectively. The quantity of catalyst used was 2.1 g and the GHSV 5625 h^{-1}. The catalyst particle diameters range from 0.45 to 0.55 mm. This allows intraparticle diffusion to be considered negligible. Tests varying feed rate at a constant *W/F* ratio indicated that diffusion of the gases through the catalyst particles was not rate controlling. The catalytic tests were carried out after 3 h of pretreatment at 400°C in the reaction medium; after this time no significant deactivation was noted in about 30 h of working time of the catalyst.

The analyses of feed and of the products of reaction were carried out using a gas chromatograph (Thermal Conductivity Detector) on line with the reactor and operating with two sequential columns (dimetylsulfolane for the analysis of 1-butene, 2-butenes, butadiene, and CO_2; molecular sieve for the separation of nitrogen, oxygen, and CO). The presence of other organic products was checked using another gas chromatograph (Flame Ionization Detector) operating at a programmed temperature with a Porapak QS column; the gas chromatograph was connected with a hot line to the reactor.

RESULTS

X-Ray Diffraction

The X-ray diffraction patterns of the SbFe 1 and SbFe 2 catalysts calcined at different temperatures are reported in Figs. 1a and b. For catalyst SbFe 2, the lines of $FeSbO_4$ rutile (*12*) [*d*,(*hkl*) = 3.28 Å(110), 2.56 Å(101) 2.32 Å(200), 1.72 Å(211), 1.64 Å(220), and 1.47 Å(310)] were still present after calcination at 350°C. Increasing the calcination temperature to 900°C caused a decrease in the linewidth to occur because

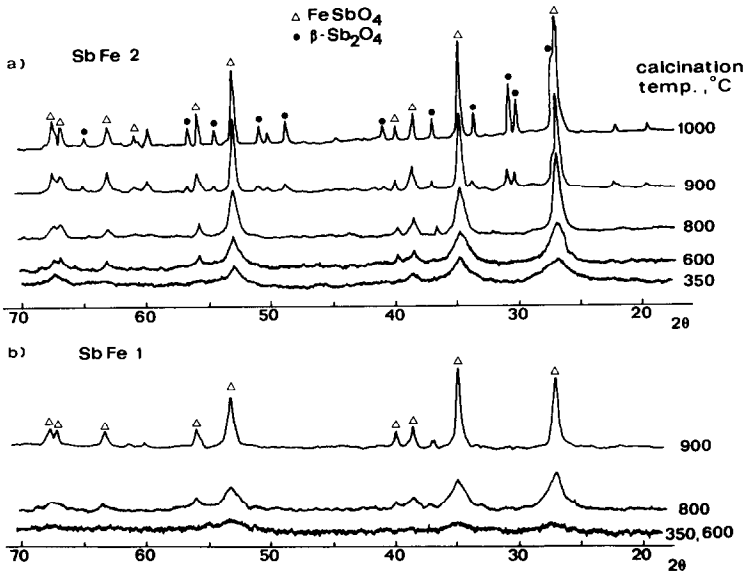

FIG. 1. X-Ray diffraction patterns of SbFe 1 and SbFe 2 as a function of calcination temperature.

of sintering of the catalyst. After calcination at 900°C, new lines appeared [d,(hkl) = 3.23 Å(110), 2.87 Å(311), and 1.86 Å(420)] due to β-Sb_2O_4; after calcination at 1000°C, the lines of β-Sb_2O_4 became relatively more intense with respect to the lines of $FeSbO_4$. The cell volume of the rutile phase of the SbFe 2 catalyst and the increase in intensity of β-Sb_2O_4 lines are reported in Fig. 2a. The cell volume was high at low calcination temperatures and with increasing calcination temperature tended toward that reported in the literature for $FeSbO_4$ rutile. After catalytic tests, no variation could be detected in the cell volume of the SbFe 2 calcined at 900°C.

In the case of SbFe 1, the $FeSbO_4$ rutile lines appeared only after calcination at 600°C. A decrease in linewidth occurred when the calcination temperature was increased to 900°C. The cell volume of SbFe 1 (Fig. 2b) is higher than the one reported in the literature; however, after catalytic tests (catalyst SbFe 1 calcined at 900°C), the cell volume became similar to that reported in the literature (*12*).

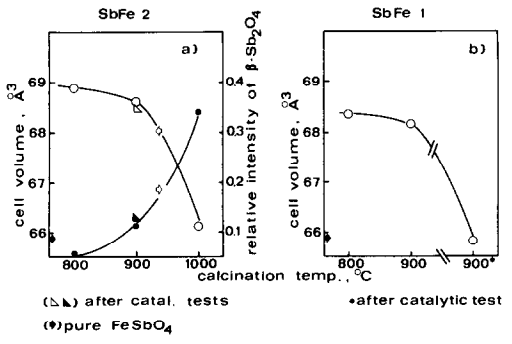

FIG. 2. (a) Cell volume and relative intensity of the (311) [β-Sb_2O_4] in respect to the (101) [$FeSbO_4$] lines for SbFe 2 as a function of calcination temperature and after catalytic tests (*12*). (b) Cell volume as a function of calcination temperature and after catalytic tests for SbFe 1.

Infrared Spectra

The infrared spectra of both SbFe 1 and SbFe 2 after calcination up to 900°C are very similar but the spectra, in particular for the catalysts calcined at low temperatures, are not well resolved. Reported in Fig. 3a are the transmission infrared spectra of the SbFe 1 and SbFe 2 catalysts calcined at 900°C. As compared with SbFe 1, catalyst SbFe 2 showed an additional weak band at about 820 cm^{-1}. This shoulder, attributed to Sb(V)=O double bond

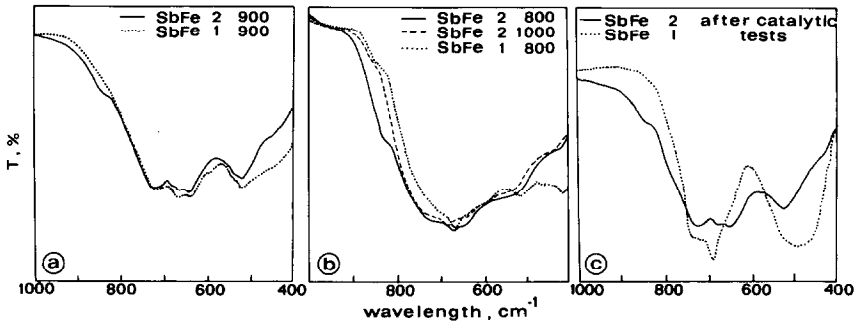

FIG. 3. (a) Infrared transmission spectra of catalysts SbFe 1 (· · ·) and SbFe 2 (—) calcined at 900°C. (b) Infrared diffuse reflectance spectra of catalysts SbFe 1 (· · ·) and SbFe 2 (—) calcined at 800°C and of catalyst SbFe 2 (– – –) calcined at 1000°C. (c) Infrared transmission spectra of catalysts SbFe 1 (· · ·) and SbFe 2 (—) calcined at 900°C after the catalytic tests with 1-butene.

streacking (*4*, *13*), is present in Sb_6O_{13} (not in α- and β-Sb_2O_4) and in a wide class of antimonates active in butadiene synthesis (USb_3O_{13} and in antimonates with trirutile structures Ni–, Mn–, and Co–Sb_2O_6) (*4*, *14*). Reported in Fig. 3b are the diffuse reflectance infrared spectra of SbFe 1 and SbFe 2 calcined at 800°C, a temperature at which X-ray diffraction analysis did not show the presence of free β-Sb_2O_4 in the catalysts. This technique, more sensitive to surface layers, showed an enhancement of the intensity of the shoulder at 820 cm^{-1} as compared to the corresponding transmission infrared spectra. After calcination at 1000°C the intensity of the shoulder at 820 cm^{-1} in SbFe 2 strongly decreased. After the catalytic tests (see Fig. 3c), the infrared spectrum of SbFe 1 calcined at 900°C changed considerably, whereas no significant modifications are noted in the spectrum of the SbFe 2 catalyst. It is worth noting that the spectrum of SbFe 1 after catalytic tests fit that reported by Rocchiccioli-Deltcheff *et al.* (*15*) for the pure $FeSbO_4$ rutile phase.

Mössbauer Analysis

Figure 4a shows the room-temperature Mössbauer spectrum of the SbFe 1 catalyst calcined at 350°C. This spectrum can be interpreted as the superposition of two quadrupole doublets, ε and η, due, respectively,

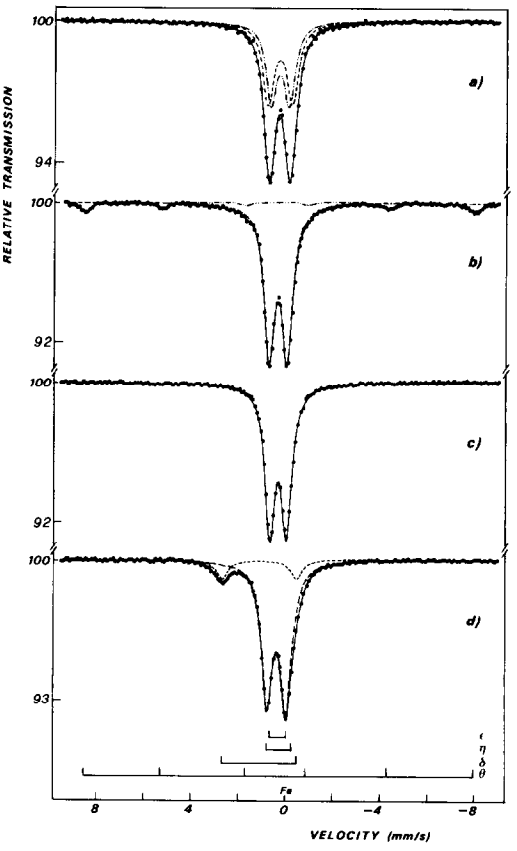

FIG. 4. Room-temperature Mössbauer spectra for SbFe 1 calcined at 350°C (a); at 900°C before catalytic tests (b); at 900°C after catalytic tests (c); for SbFe 2 calcined at 350°C (d).

to high-spin Fe^{3+} in distorted octahedral sites of $FeSbO_4$ (*16*) and to Fe^{3+} in the paramagnetic state in small particles of α-Fe_2O_3 (*7, 17, 18*). In agreement with this, low-temperature measurements for the same sample show the ε doublet and weak Fe_2O_3 Zeeman lines. With increasing calcination temperature, the average particle size of hematite increases, reaching, for T = 900°C, a value which almost corresponds to a pure ferromagnet. Figure 4b shows the room-temperature Mössbauer spectrum measured for SbFe 1 calcined at 900°C. Both the quadrupole doublet relative to $FeSbO_4$ and the ϑ sextet corresponding to ferromagnetic α-Fe_2O_3 contribute to this spectrum. Figure 4c reports the spectrum measured for the same sample of Fig. 4b after the catalytic tests in which no contribution due to α-Fe_2O_3 could be detected.

All the room-temperature Mössbauer spectra measured for SbFe 2 catalysts calcined at different temperatures from 350°C (Fig. 4d) to 1000°C can be interpreted as the superposition of two quadrupole doublets; a low intense one (δ) which can be attributed to octahedral high-spin Fe^{2+} ions and a predominant one (ε) which can be attributed to distorted octahedral high-spin Fe^{3+} of the $FeSbO_4$ mixed oxide. The relative quadrupole splittings, isomer shifts, and linewidths as a function of the calcination temperature are reported in Fig. 5. In this case, neither the low-temperature measurements nor the spectra of high-temperature calcination samples gave indication of the presence of iron oxides in the catalysts. No differences were detected in the spectra measured before and after tests for SbFe 2 calcined at 900°C.

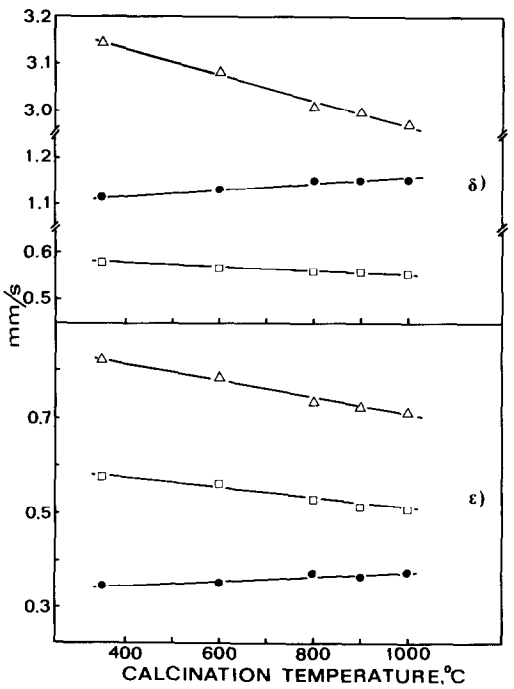

FIG. 5. Quadrupole splitting (△), isomer shift (●), and linewidth (□) for SbFe 2 as a function of calcination temperature.

Catalytic Activity

The yield in butadiene, in carbon oxides, and the conversion in 1-butene oxidation as a function of the reaction temperature are reported in Fig. 6 for two samples (SbFe 1 and SbFe 2) calcined at 900°C. The calcination at high temperatures was necessary to obtain a decrease in the surface area from 150 m^2/g to a value of 7 m^2/g; both catalysts calcined at 900°C had about the same surface area.

The catalyst SbFe 2 was active at very low temperatures and showed a strong increase in activity and in selectivity in butadiene formation as compared with SbFe 1. No other products of partial oxidation were detected except for traces of furan. The catalysts did not present isomerization properties (2-butenes formation) and therefore probably no acid sites were present on the surface.

DISCUSSION

Formation of a Nonstoichiometric (NS) Rutile Structure

X-Ray diffraction analysis shows that when SbFe 2 is calcined at $T \geq 900$°C, β-Sb_2O_4 is present together with $FeSbO_4$ rutile, whereas at lower calcination temperatures only the lines of a rutile structure can be detected. Therefore the question is

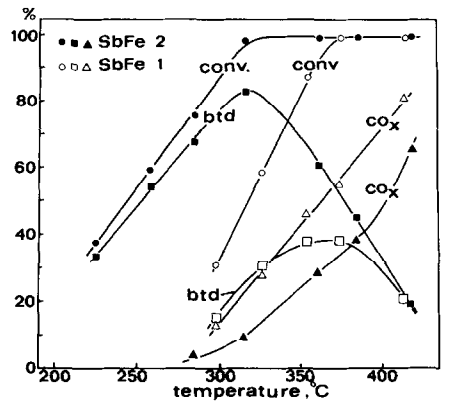

FIG. 6. Catalytic behavior of SbFe 1 and SbFe 2. btd, Yield of butadiene; conv, conversion; and CO_x, yield of carbon oxides. Experimental conditions: 0.606 vol% 1-butene, 11.1 vol% oxygen; weight of catalyst 2.1 g; GHSV 5625 h^{-1}.

where is the excess antimony located at $T < 900$°C. With increasing calcination temperature, the cell volume of rutile decreases to a value of pure $FeSbO_4$ (Fig. 2a) and correspondingly, the quadrupolar splitting and the linewidth in the Mössbauer spectra (Fig. 5) also decrease. These results suggest that the excess of antimony (in respect to the ratio 1) is located inside the rutile structure. Antimony oxide can form only at very high calcination temperatures and this suggests that antimony is held strongly within the structure. X-Ray diffraction data (Fig. 2b) indicated that the catalysts present a deformed rutile structure. In addition, the Mössbauer spectra also show the presence of α-Fe_2O_3 (Fig. 4b). These results suggest that also in the case of catalysts with a 1 : 1 ratio, a NS-rutile structure with excess antimony is present. The amount of iron in the α-Fe_2O_3 should correspond to the amount of antimony within the rutile structure. The fact that even at high temperatures no solid state reaction occurs between α-Fe_2O_3 and the excess antimony confirms that this kind of antimony is held strongly inside the rutile structure itself.

Role of Method of Preparation

The catalysts were prepared by coprecipitation in a basic medium where the antimony is present as condensed antimonate (*19*) such as $[Sb_2O_6(OH)]^{3-}$. Assuming that the anion which precipitates is a condensed antimonate, the precipitate should contain an Sb : Fe ratio greater than 1. Therefore, independently from the starting Sb : Fe ratio, both SbFe 1 and SbFe 2 should contain the same compound. After calcination up to 800°C, this gave rise to the formation of NS-rutile containing excess antimony in both cases.

Nature of Active Sites

Catalytic data (Fig. 6) illustrated that the excess antimony is a strong promoter of activity and selectivity in allylic oxidation (butadiene formation). The analyses of the structure show that before catalytic tests, a NS-rutile with excess antimony is present in both catalysts; after reaction, SbFe 1 is transformed to pure $FeSbO_4$ whereas the NS-rutile is still present in the SbFe 2. This transformation is particularly evident in the infrared spectra (Fig. 3c). Because the samples were stabilized for 3 h in the reaction medium at 400°C before making the catalytic tests, the two catalytic behaviors can be assigned to the pure $FeSbO_4$ (SbFe 1) and to the NS-rutile with excess antimony (SbFe 2). Therefore, the inclusion of excess antimony in the rutile structure leads to the formation of new very active and selective centers for allylic oxidation.

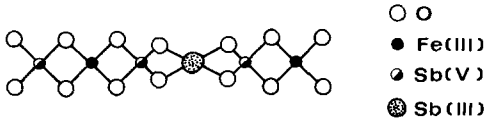

The antimony can be located either in substitutional positions of Fe(III) or in interstitial positions. From our data it is not possible to distinguish between these two possibilities but probably, because of the high quantities of antimony that can be included in the rutile structure, both mechanism are operating. In particular, the sub-

stitution of Fe(III) with Sb(III) in the rutile oxygen octahedra probably also deforms the neighboring octahedra due to the larger size of the Sb(III) ionic radius and thus increases the cell volume. Therefore it is possible to explain the deformation of octahedral sites of Fe(III) as shown by Mössbauer analysis and the expansion of the cell volume shown by X-ray diffraction analysis. The simultaneous presence of Sb(V) and Sb(III) in $FeSbO_4$ with excess antimony also is confirmed by XPS analysis (*6*). Confirming the results of Aso *et al.* (*5, 6, 10*) and Burriesci *et al.* (*7, 9*) we also found the presence of Fe(II) in the catalysts with an Sb : Fe ratio of 2. However, these authors suggest that the Fe(II) is related to the formation of a surface compound with Sb : Fe = 2 (*5, 6, 10*) or derives from the antimony held within the structure (in interstitial positions) according to charge balance (*7*). Our data suggested that only very small amounts of Fe(II) are formed in SbFe 2 catalysts (Fig. 4d) and therefore the predominant effect is the formation of an Sb(III)–Sb(V) rutile-like structure held within the $FeSbO_4$ rutile structure. Infrared diffuse reflectance spectra (Fig. 3b) indicated the presence of Sb(V)=O groups on top layers of SbFe 2 catalysts calcined at 800°C; after calcining at 1000°C, the same catalyst showed a strong decrease of the absorption at 820 cm^{-1} and thus of the number of antimony–oxygen double bonds. In the same range of calcination temperatures, X-ray diffraction analysis showed the transformation of SbFe 2 from the NS-rutile structure to pure rutile and β-Sb_2O_4. This suggests that the NS-rutile structure is characterized by the presence of Sb(V)=O groups on the surface. Open channels are present in the rutile structure with radii of about 0.77 Å along the *c* axis (*20*). This gives rise to a situation on the surface of the rutile as shown in Fig. 7. Sb(V) (radius about 0.60 Å) can be located on the surface in these interstitial sites. Two oxygen atoms are present in the neighborhood of this antimony atom; the antimony–oxygen distance is consistent with that of a double bond. This simplified model suggests that the excess antimony on the surface is located in very particular positions creating surface groups such as O=Sb=O. In previous studies, Trifirò *et al.* (*4, 21–23*) suggest the fundamental role of the presence of two geminate Sb=O double bond groups or in general of two contiguous M=O double bonds in the allylic oxidation reactions. This hypothesis is in agreement with the results recently reviewed by Grasselli *et al.* (*24, 25*) on the mechanistic features of selective oxidation and ammoxidation catalysts. It is worth noting that the proposed model is in agreement with the surface situation of the trirutile structure ($FeSb_2O_6$), as previously proposed by Trifirò and Sala (*4*) and by Aso *et al.* (*5, 6*). Furthermore other antimonates with the trirutile structure (Ni–, Mn–, Co–Sb_2O_5) were found to be highly selective in butadiene formation (*4*).

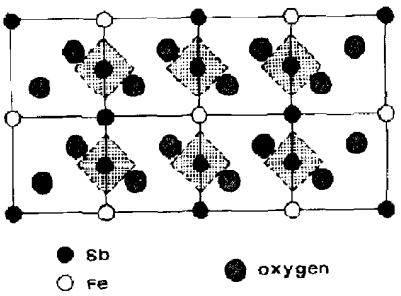

FIG. 7. Disposition of ions on the surface of the NS-rutile structure. Dashed lines indicated the open channels along the *c* axis in the rutile structure (*20*).

In conclusion, the formation of these surface groups due to the inclusion of Sb inside the rutile structure can explain the observed increase in activity and selectivity in SbFe 2.

ACKNOWLEDGMENT

This work was supported by the contribution from the "Ministero Pubblica Istruzione," Rome (Italy).

REFERENCES

1. Boreskov, G. K., Vent'yaminov, S. A., Dzis'ko, V. A., Tarasova, D. V., Dindoin, V. M., Sazonova, M. M., Olen'kova, T. P., and Kelefi, L. M., *Kinet. Catal.* **10,** 1350 (1969).

2. Shchukin, V. P., Boreskov, G. K., Ven'yaminov, S. A., and Tarasova, D. V., *Kinet. Catal.* **11,** 153 (1970).
3. Fattore, V., Furhman, Z. A., Manara, G., and Notari, B., *J. Catal.* **37,** 223 (1975).
4. Sala, F., and Trifirò, F., *J. Catal.* **41,** 1 (1976).
5. Aso, I., Furukawa, S., Yamazo, N., and Seiyama, T., *J. Catal.* **64,** 29 (1980).
6. Aso, I., Amomoto, T., Yamazoe, N., and Seiyama, T., *Chem. Lett.* 365 (1980).
7. Burriesci, M., Garbassi, F., Petrera, M., and Petrini, G., *J. Chem. Soc. Faraday Trans. 1* **78,** 817 (1982).
8. Kriegsmann, H., Ohlmann, G., Sheve, J., and Ulrich, F. J., *in* "Proceedings, 6th International Congress on Catalysis, London, 1976." (G. C. Bond, P. B. Wells, and F. C. Tompkins, Eds.), p. 836. The Chemical Society, London, 1976.
9. Petrera, M., Gennaro, A., Burriesci, M., and Bart, J. C. P., *Z. Anorg. Allg. Chem.* **472,** 179 (1981).
10. Yamazoe, N., Aso, I., Anamoto, T., and Seiyama, T., "Proceedings, 7th International Congress on Catalysis, Tokio, 1980," Part B, p. 1239. Elsevier, Amsterdam, 1981.
11. Dziewiecki, Z., and Makowski, A., *React. Kinet. Catal. Lett.* **1,** 51 (1980).
12. Korinth, J., and Roye, P., *Z. Anorg. Allg. Chem. B* **340,** 146 (1965).
13. Adamiya, T. V., Mishchenko, Yu. A., Dulin, D. A., and Gel'bsthein, A. I., *Kinet. Catal.* **11,** 970 (1970).
14. Sala, F. and Trifirò, F., *J. Catal.* **34,** 68 (1974).
15. Rocchiccioli-Deltcheff, C., Dupuis, T., Frank, R., Harmelin, M., and Wadier, C., *C. R. Acad. Sci. Paris B* 541 (1970).
16. Bartenev, G. M., Zakirov, R. R., and Tsyganov, A. D., *Sov. Phys. Solid State* **16,** 2409 (1975).
17. Van der Kraan, A. M., *Phys. Status Solidi* **18,** 215 (1973).
18. Krupyanskii, Yu. F., and Suzdalev, I. P., *Sov. Phys. JETP (Engl. Transl.)* **38,** 859 (1974).
19. Pascal, P. (Ed.), "Nouveau Traitè de Chinmie Minérale," Tome XI, p. 609. Masson, Paris, 1958.
20. Matzke, H., *in* "Nonstoichiometric Oxides" (O. T. Søresen, Ed.), p. 160. Academic Press, New York/London, 1981.
21. Mitchell, P. C. H., and Trifirò, F., *J. Chem. Soc. (A)* 3183 (1970).
22. Trifirò, F., Centola, P., and Pasquon, I., *J. Catal.* **1,** 86 (1968).
23. Trifirò, F., and Pasquon, I., *J. Catal.* **4,** 412 (1968).
24. Grasselli, R. K., and Burrington, J. D., "Advances in Catalysis," Vol. 30, p. 133. Academic Press, New York, 1981.
25. Grasselli, R. K., Burrington, J. D., and Brazdil, J. F., *Faraday Discuss.* **72,** 203 (1981).